

# Hip Motion Analysis Using Multi Phase (Virtual and Physical) Simulation of the Patient-specific Hip Joint Dynamics

Yoshito OTAKE<sup>a,1</sup>, Naoki SUZUKI<sup>a</sup>, Asaki HATTORI<sup>a</sup>, Hidenobu MIKI<sup>b</sup>, Mitsuyoshi YAMAMURA<sup>c</sup>, Kazuo YONENOBU<sup>d</sup>, Takahiro OCHI<sup>e</sup>, Nobuhiko SUGANO<sup>f</sup>

<sup>a</sup>*Institute for High Dimensional Medical Imaging, Jikei University School of Medicine  
4-11-1, Izumi Honcho, Komae-shi, 201-8461, Tokyo, Japan*

<sup>b</sup>*Osaka National Hospital  
2-1-14 Houenzaka, Chuo-ku, 540-0006, Osaka, Japan*

<sup>c</sup>*Kyowa-kai Hospital*

*1-24-1 Kishibe-kita, Suita 564-0001, Osaka, Japan*

<sup>d</sup>*Department of Orthopaedic Surgery, Osaka Minami National Hospital  
2-1 Kidohigasi-machi, Kawachinagano 586-0008, Osaka, Japan*

<sup>e</sup>*Sagamihara National Hospital*

*18-1 Sakuradai, Sagamihara-shi, 228-8522, Kanagawa, Japan*

<sup>f</sup>*Department of Orthopaedic Surgery, Osaka Univ. Grad. Sch. of Med.  
2-2 Yamadaoka, Suita 565-0871, Osaka, Japan*

**Abstract.** In total hip arthroplasty (THA), the patient-specific bone geometry or the characteristics of the skeletal movement should be considered during treatment in order to prevent complications. In this paper, we propose a novel approach for the analysis of joints which combines the patient-specific virtual and physical simulation. The patient-specific anatomical structure and hip motion was obtained from CT and optical motion capture. The virtual simulation was conducted by integrating these data using virtual reality technique. The physical simulation was achieved by using plaster models of the patient's pelvis and femur and robotic manipulator. The plaster models were driven by two robotic manipulators to reproduce the hip motion. The accuracy of the robot movement was 0.245mm over the working area according to the validation by an optical tracking system. By combining this system with linear actuators that reproduce the muscle functions, patient-specific muscle function can be simulated, thereby helping clinicians to diagnose and make a treatment plan.

**Keywords.** total hip arthroplasty, virtual simulation, physical simulation

## 1. Introduction

Total hip arthroplasty (THA) is a surgical procedure in which the diseased parts of the hip joint are removed and replaced with new artificial ones. The main complications of this surgery are dislocation and loosening due to the wearing of the sliding surface. To

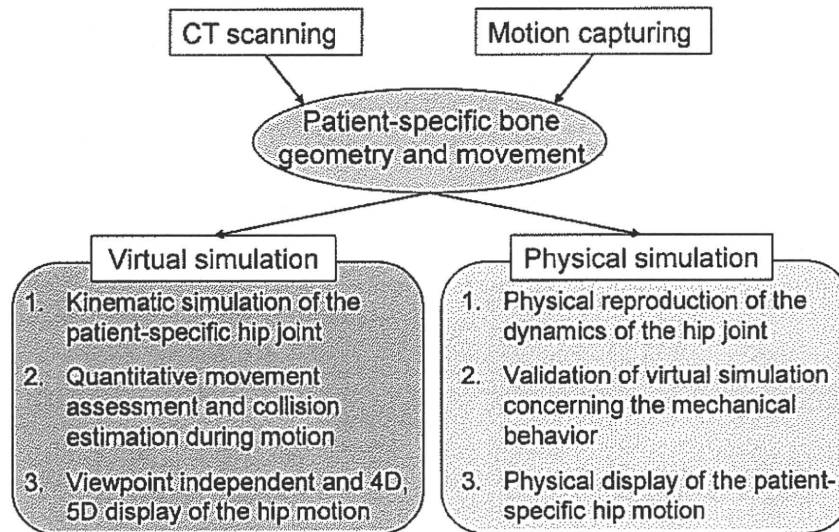


Fig. 1 Overview of the proposed system

prevent these complications, the patient-specific bone geometry or the characteristics of the skeletal movement should be considered during treatment. In recent studies [1][2], a patient-specific three-dimensional (3D) skeletal model prepared from computed tomography (CT) and motion capture data of the patient was used to simulate patient-specific skeletal motion. On the other hand, for analyzing the typical dynamics of joints, especially the knee joint, a few researchers have developed systems that reproduce previously recorded 6-degree-of-freedom kinematics using a robotic manipulator with the joint part of porcine carcasses or cadavers [3][4]. These systems were intended to be used for the analysis of the general characteristics of a dynamic state of the knee joint such as the tension in the anterior cruciate ligament, etc. However, because these systems used a porcine carcass or a cadaver, the motion of the individual was not available: therefore the simulation result has some limitations concerning the correspondence between the geometry and the movement.

In this paper, we propose a novel approach for the analysis of joints which combines the patient-specific virtual simulation we have been developing for patients after THA [2] and a newly developed physical simulation system. As described above, physical simulation in this research analyzes the dynamics of the joint such as forces acting on or within the joint. This physical simulation system consists of a 6-degree-of-freedom robotic manipulator and a plaster model of the patient-specific bone geometry. Analysis by this physical simulation reinforces the result of virtual simulation and also helps the patients to understand the motion of their hip joint.

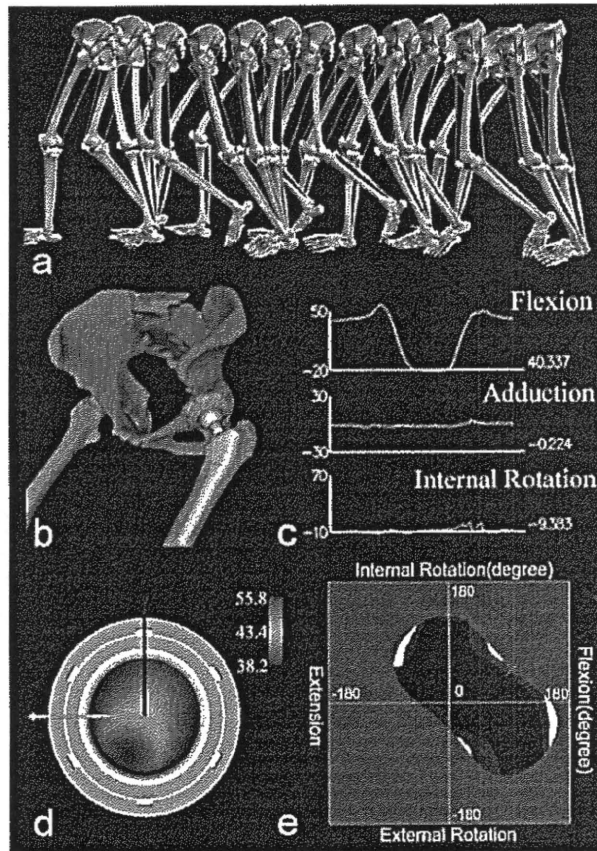


Fig. 2 Simulation using the virtual model. a, b: skeletal motion analysis; c: transition of the joint angle; d: distribution of the wearing part estimated by the simulation; e: estimated range of motion.

## 2. Methods

First, we scanned the patient's lower extremity using CT and constructed a patient-specific 3D bone geometry model. Then, we captured the motion of the patient during some daily activities. The details of the method for obtaining these patient-specific data were described in the previous paper [2]. These data were used as the input for both the virtual and physical simulation systems (Fig. 1). In the virtual simulation system, accurate joint motion, collisions between hard tissue around the hip joint, and the estimated muscle force induced by the surrounding muscles were calculated (Fig. 2).

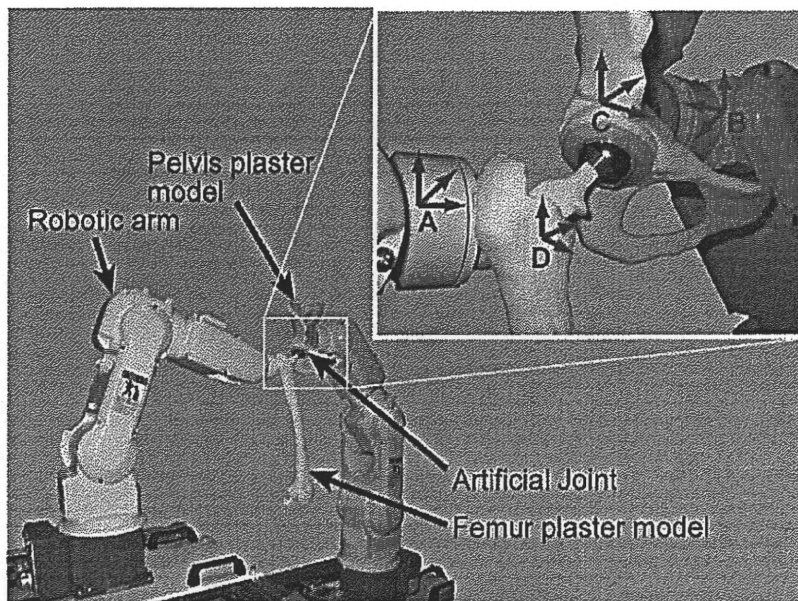


Fig. 3 Configuration of the physical simulation system. It reproduces the patient-specific bone geometry and the motion of the hip joint.

The physical simulation system was created as follows. First, we manufactured a plaster model from the patient-specific bone geometry data of the pelvis and femur by using a laminate molding technique (layer thickness: 0.1 mm). The plaster models were hardened by a certain type of plastic to obtain similar strength as human bone. In addition, the real artificial joint, which is the spherical metal head of a femur and the polyethylene cup, was combined with the plaster model to duplicate the sliding condition of the patient's hip joint. Then, each plaster model was mounted on the serial-articulated robotic manipulator (Fig. 3). Both robotic manipulators were registered by an optical tracking device, OPTOTRAK system (NDI Inc., Canada), and the relative position was calculated. Both robots were driven simultaneously by a single computer according to the patient's motion data to reproduce the relative motion between pelvis and femur.

Then, to validate the accuracy of the robot movement, the programmed movement of the robotic arm was validated using an optical tracking device. The robot with optical markers was driven throughout the working area (Fig. 4). The distance between the programmed and measured position was calculated as the error.

### 3. Results

Using the virtual and physical simulation system, the patient-specific movement of the skeletal structures was reproduced (Fig. 5). This helped the clinician in the analysis of the

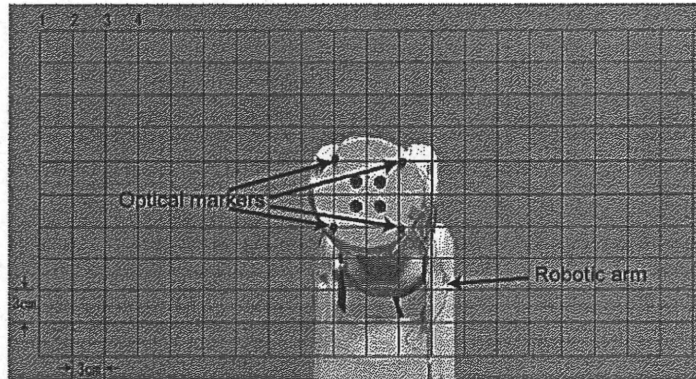


Fig. 4 Experiment for validating the accuracy of the robot manipulator. The red grid indicates the position that the experiment targeted.

joint structure and the dynamics of each patient's hip joint in detail, such as the contact force at the sliding surface or the characteristics of the movement. The root-mean-square error between the programmed and measured motion was 0.245 mm over the working area.

#### 4. Conclusions

In this paper, we proposed a new approach for the analysis of joint motion and determined its feasibility. As described in previous research, physical simulation using the real joint object is extremely important for analyzing the forces acting on or within joints; however until now this has been achieved only for nonliving bodies. In the proposed system, even though only a few parts such as bones, artificial joints and motions were reproduced, it used data from living patients. For the application of these types of simulation to actual clinical settings for diagnosis, surgical planning or treatment planning, etc., the simulation of each patient's joint is inevitable. Furthermore, by combining this system with linear actuators that reproduce the muscle functions and a 6-axis force sensing device, patient-specific muscle function can be simulated accurately, thereby helping clinicians to select the optimal size of the artificial joint in preoperative planning and also predict postoperative complications such as dislocation or wearing at the sliding surface.

#### References

1. Y.Otake, K.Hagio, N.Suzuki, A.Hattori, N.Sugano, K.Yonenobu, T.Ochi: Four-dimensional Lower Extremity Model of the Patient after Total Hip Arthroplasty, *Journal of Biomechanics*, vol.38, pp.2397-405, 2005.

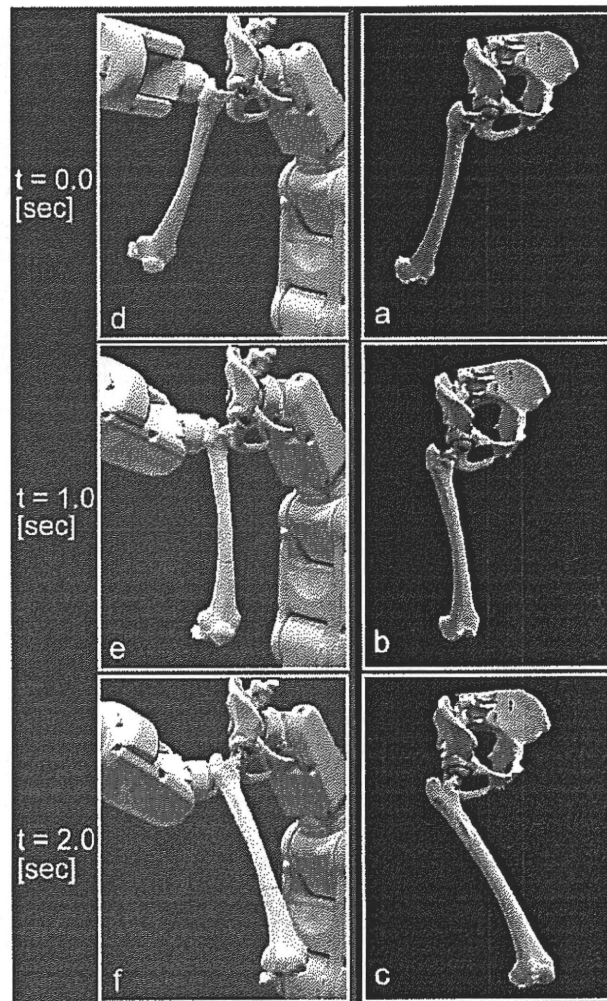


Fig. 5 Result of the virtual and physical simulation. a-c: display of the movement of the virtual model, d-f: motion of the plaster model and the robotic manipulator.

2. Y. Otake, N. Suzuki, A. Hattori, H. Miki, M. Yamamura, N. Nakamura, N. Sugano, K. Yonenobu, T. Ochi: Estimation of Dislocation after Total Hip Arthroplasty by 4-Dimensional Hip Motion Analysis, *Studies In Health Technology and Informatics* vol.111, pp.372-7, 2005.
3. Susan M. Moore, Maribeth Thomas, Savio L-Y. Woo, Mary T. Gabriel, Robert Kilger, Richard E. Debski: A novel methodology to reproduce previously recorded six-degree of freedom kinematics on the same diarthrodial joint, *Journal of Biomechanics* vol.39, pp. 1914-23, 2006.
4. Shon P. Darcy, Robert H. P. Kilger, Savio L-Y. Woo, Richard E. Debski: Estimation of ACL forces by reproducing knee kinematics between sets of knees: A novel non-invasive methodology, *Journal of Biomechanics* vol.39, pp. 2371-7, 2006.

## Evaluation of cartilage matrix disorders by T2 relaxation time in patients with hip dysplasia

T. Nishii M.D.†\*, H. Tanaka M.D.‡, N. Sugano M.D.†, T. Sakai M.D.†,

T. Hananouchi M.D.† and H. Yoshikawa M.D.†

† Department of Orthopaedic Surgery, Osaka University Medical School E3, 2-2 Yamadaoka, Suita, Osaka 565-0871, Japan

‡ Department of Radiology, Osaka University Medical School, 2-2 Yamadaoka, Suita, Osaka 565-0871, Japan

### Summary

**Objective:** Early detection of cartilage disorder in dysplastic hips is important in predicting subsequent progression of osteoarthritis and determining the appropriate timing of osteotomy surgery. We assessed the feasibility of T2 assessment using magnetic resonance (MR) imaging at 3 T for evaluating early changes in the acetabular and femoral cartilages for patients with hip dysplasia.

**Methods:** Sagittal T2 maps of the hip were obtained using 3 T MR imaging in 10 normal volunteers (14 hips) and in 23 patients (26 hips) with hip dysplasia at pre-arthritis stage (without osteoarthritis) or early-arthritis stage (with osteoarthritis at the Kellgren–Lawrence system of grade 1 or 2). T2 values and the visual appearance of T2 mapping, including gradient T2, low T2, and high T2 patterns, were compared at the superior zones of the acetabular and femoral cartilages among the normal, pre-arthritis, and early-arthritis groups.

**Results:** There were no significant differences in T2 values for both cartilages among the three groups. Regarding the visual appearance of T2 mapping for the acetabular cartilage, all hips in the normal group showed a gradient T2 pattern, while the pre-arthritis groups included six hips (43%) with a low T2 pattern, and the early-arthritis group showed either a low T2 pattern (33%) or a high T2 pattern (67%). The frequency of the gradient T2 pattern was significantly lower for dysplastic hips than for normal hips, in the acetabular and femoral cartilages ( $P < 0.05$ ).

**Conclusions:** This preliminary study demonstrated the clinical feasibility of T2 assessment of hip cartilage using 3 T MR imaging. T2 mapping classification may enable the early detection of osteoarthritic degeneration and the detection of developmental disorders of cartilage matrix in patients with hip dysplasia.

© 2007 Osteoarthritis Research Society International. Published by Elsevier Ltd. All rights reserved.

**Key words:** Hip dysplasia, MR imaging, Cartilage, T2 relaxation time, Osteoarthritis, Cartilage matrix.

### Introduction

Hip dysplasia is one of the major causes of hip osteoarthritis<sup>1,2</sup>. Radiological evidence of dysplasia in hips without osteoarthritis is shown as a risk factor for the development of hip osteoarthritis in a prospective study<sup>3</sup>. Hips with moderate or severe degrees of dysplasia are likely to deteriorate progressively and eventually develop into terminal osteoarthritis with persistent symptoms and severely impaired function<sup>4</sup>. When effective surgical treatment such as osteotomy surgery is applied before osteoarthritic changes progress, reliable outcomes can be expected, with the prevention of osteoarthritic changes; however, delay of treatment following osteoarthritic involvement often results in unsatisfactory outcomes<sup>5</sup>. Early detection of cartilage disorders in dysplastic hips is important in predicting the subsequent progression of osteoarthritis and determining appropriate timing for osteotomy surgery.

Several imaging modalities are currently available to evaluate osteoarthritis of the hip, including plain radiography, arthrography, bone scintigraphy<sup>6</sup>, computed tomography (CT) arthrography<sup>7</sup>, and magnetic resonance (MR) imaging with and without arthrographic effect<sup>8,9</sup>. Plain radiography is widely used for diagnosis and assessment of the severity of joint osteoarthritis, and showed significant correlation with hip cartilage thickness and volume<sup>10</sup>; however, several other reports have proposed inaccurate relationships between radiographic findings and the status of the articular cartilage<sup>11,12</sup>. Recent investigations using CT arthrography<sup>7</sup> and MR imaging with and without arthrographic effect<sup>7–9</sup> achieved excellent visualization and sensitive detection of morphological changes in hip cartilage (thinning or defect); however, the diagnostic abilities of these modalities are limited for early cartilage disorders without change of cartilage thickness or volume, such as softening and surface fibrillation<sup>7</sup>. Disruption or alteration of the cartilage matrix such as a decrease in the concentration of proteoglycan and an increase in water content is found histologically in early changes of osteoarthritis<sup>13</sup>. It may be more effective to image cartilage matrix disorders or water content than to image cartilage morphological changes such as thickness and shape in detecting early changes of cartilage disorders with high sensitivity and accuracy.

\*Address correspondence and reprint requests to: Takashi Nishii, M.D., Department of Orthopaedic Surgery, Osaka University Medical School E3, 2-2 Yamadaoka, Suita, Osaka 565-0871, Japan. Tel: 81-6-6879-3552; Fax: 81-6-6879-3559; E-mail: nishii@ort.med.osaka-u.ac.jp

Received 24 December 2006; revision accepted 5 June 2007.

MR imaging techniques that have been proposed for sensitive evaluation of cartilage matrix changes include T2 relaxation time (T2), delayed gadolinium-enhanced MR imaging of cartilage (dGEMRIC), and T1 in the rotating frame (T1rho)<sup>14</sup>. Evaluation of T2 of the articular cartilage shows great potential for the quantitative assessment of collagen and water content<sup>15,16</sup> and indicates clinical usefulness for knee imaging *in vivo*<sup>17,18</sup>; however, to the best of our knowledge there have been no reports that assess hip cartilage by T2. This is because of difficulties involved in obtaining satisfactory image quality and in differentiating between the acetabular and femoral cartilages.

MR imaging at higher magnetic field strength (at 3 T or more) may provide improved image quality of the hip cartilage due to superior signal-to-noise contrast<sup>19</sup>. The objective of the present study is to assess the feasibility of T2 evaluation using MR imaging at 3 T in detecting early changes in the acetabular and femoral cartilages in patients with hip dysplasia.

## Materials and methods

Ten normal volunteers (14 hips) and 23 patients with hip dysplasia (26 hips) were included in this study. Because patients with hip dysplasia are predominantly female<sup>20</sup>, men were excluded from the study to prevent the potentially confounding influence of sex difference on T2 in the articular cartilage<sup>21</sup>. Exclusion criteria for volunteers were present and/or past experience of hip pain, stiffness, or gait disability. Hip dysplasia was defined by center-edge angle of Wiberg of 24° or less<sup>22</sup> on anteroposterior radiographs. Inclusion criteria for dysplastic hips to the study were as follows: no previous hip surgery, Class I subluxation (less than 50%) according to the classification of Crowe *et al.*<sup>23</sup>, and radiological osteoarthritis classification according to the Kellgren–Lawrence system<sup>24</sup> of grade 0 (no osteoarthritic finding), grade 1 (possible narrowing of joint space and/or osteophytes), or grade 2 (definite narrowing of joint space, definite osteophytes, and slight sclerosis). In the present study, osteoarthritis classification of grade 0 with radiological evidence of hip dysplasia was categorized as pre-arthritis stage, and grade 1 or 2 as early-arthritis stage. Institutional review board approval was obtained for this study, and all patients provided informed consent after the nature of the procedure had been fully explained.

The average ages of the volunteers and patients were 34 years (range, 23–51 years) and 40 years (range, 22–69 years), respectively. The average heights and weights were 163 cm (range, 153–171 cm) and 54 kg (range, 47–80 kg) in the volunteers, and 157 cm (range, 149–163 cm) and 53 kg (range, 42–80 kg) in the patients, respectively. The center-edge angle of the patients ranged from –20° to 24° (mean, 6.5°); there were 14 hips at the pre-arthritis stage (grade 0) and 12 hips at the early-arthritis stage (eight hips at grade 1 and four hips at grade 2). Patients had no pain in six hips and slight or moderate pain either while walking or after a long walk in 20 hips. The six asymptomatic hips were diagnosed as hip dysplasia during examination of the opposite symptomatic hips.

MR imaging of the hip was performed on a Signa 3 T MR scanner (GE Healthcare, WI, USA) using a flexible surface coil. The volunteers and patients were positioned supine with the hip in neutral position. Two-dimensional dual-echo spin-echo images were obtained with the following parameters: repetition time/echo time 1500 ms/10 and 45 ms; field of view 16 cm; matrix 512 × 256 interpolated to

512 × 512 with a resulting in-plane pixel resolution of 312.5 μm; 5 mm slice thickness, and two signals acquired for a total time of 13.5 min. Frequency encoding was head to foot across the hip joint, and the fat-suppression technique was used to minimize chemical shift artifact at the bone/cartilage interface. A single sagittal image passing through the center of the femoral head was obtained. When the imaging plane was lateral to the outer edge of the acetabular rim in the coronal scout view, the imaging plane was moved medially to be located within the acetabular rim. The sagittal plane was employed because cartilage disorder is often observed at the anterosuperior region of the acetabulum in arthroscopic studies of dysplastic hips<sup>25</sup>. A single slice sequence was used to prevent inaccuracy of T2 measurement caused by magnetization transfer contrast from off-resonance radiofrequency irradiation found in multi-slice sequences<sup>26,27</sup>.

The acetabular and femoral cartilages were manually segmented on the mid-sagittal image and the T2 value was calculated assuming a single exponential decay component. A color-coded T2 map of the cartilage was overlaid on the mid-sagittal image; low T2 values were represented in red while high T2 values were colored green or blue (Fig. 1). Regions of interest (ROIs) in the acetabular and femoral cartilages were defined at the weight-bearing area of the superior 20° range of the cartilage, from the cartilage surface to the basal area, and the average T2 value and visual appearance of T2 mapping within the ROIs were evaluated. The visual appearances of T2 mapping were classified into three patterns (Fig. 2): "gradient T2 pattern" for low T2 values at the deep cartilage area and high T2 values at the superficial cartilage area, which was considered representative of the spatial variation of normal knee cartilage<sup>28</sup>; "low T2 pattern" for ROIs occupied predominantly by low T2 values up to the superficial cartilage area; and "high T2 pattern" for ROIs occupied predominantly by high T2 values even at the deep cartilage area. On assessment for each case, representative cases of the three mapping patterns (Fig. 2) were used as the reference atlas. Definitions of the ROIs were repeated three times by a single observer (TS) without knowledge of presence of hip dysplasia or the radiological osteoarthritis classification, and the T2 values of the ROIs were averaged. Inter-observer reliability between two observers (TN, TS) was assessed in the first 10 subjects, with a coefficient of variation of 2.5% for the acetabular ROI and 3.8% for the femoral ROI. Visual appearance of T2 mapping was interpreted blindly by two observers (TN, TS) independently without knowledge of presence of hip dysplasia or the radiological osteoarthritis classification. In general (95% of the cases in the acetabular cartilage and 93% of the cases in the femoral cartilage), there was agreement between the two observers. In the remaining cases, a consensus of opinion was obtained between the two observers. All imaging analysis was conducted using Beth Israel Deaconess Medical Center software for functional imaging of cartilage (Boston, MA, USA).

Clinical symptoms of the hip were evaluated using the Western Ontario and McMaster Universities Osteoarthritis (WOMAC)<sup>29</sup> pain score at the time that MR imaging was conducted. When both hips were examined, WOMAC questionnaires were taken separately for the right and left hips. The WOMAC pain score was calculated as a summation of the scores ranging from 0 (no pain) to 4 (extreme pain) in response to each of five items (range of possible total score 0–20). T2 value and the visual appearance of T2 mapping for each ROI were compared among the normal,



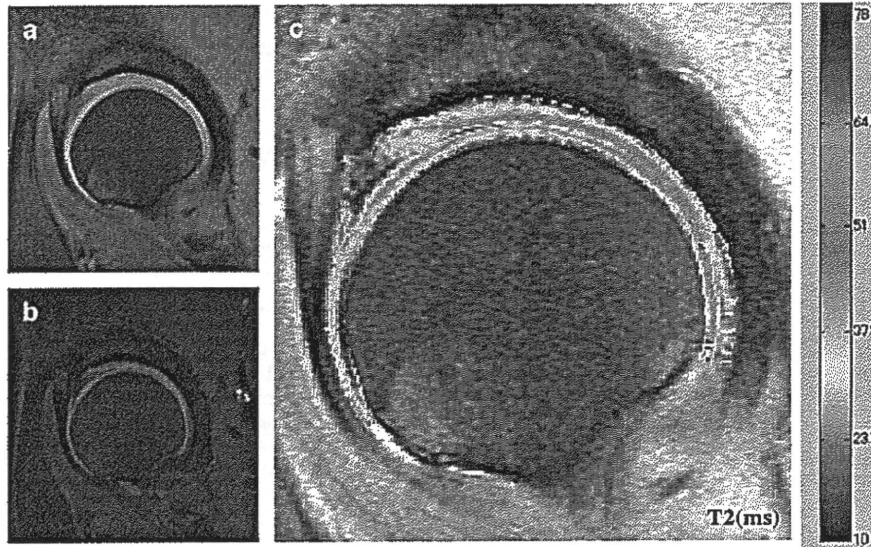


Fig. 1. Representative mid-sagittal MR images of a normal volunteer hip (a: 1500/10 ms, b: 1500/45 ms), and corresponding T2 map overlaid on the cartilage region (c). Superior and anterior directions of the hip are toward the top and left of each image, respectively.

pre-arthritis, and early-arthritis hips, using analysis of variance and the Fisher exact test. They were also compared between asymptomatic and symptomatic hips, using the nonparametric Mann–Whitney *U* test and the Fisher exact test. Between normal hips and dysplastic hips, and between asymptomatic hips and symptomatic hips, we calculated a sample size to detect a 10% difference of T2 value based

on a previous report comparing T2 value in healthy knees and osteoarthritic knees<sup>18</sup>. Fourteen hips or more in each group were sufficient to determine whether there was a significant difference (power > 0.8,  $P < 0.05$ ). The relationship between WOMAC pain scores and T2 values was evaluated using the Spearman correlation coefficient. A *P* value of less than 0.05 indicated significance.

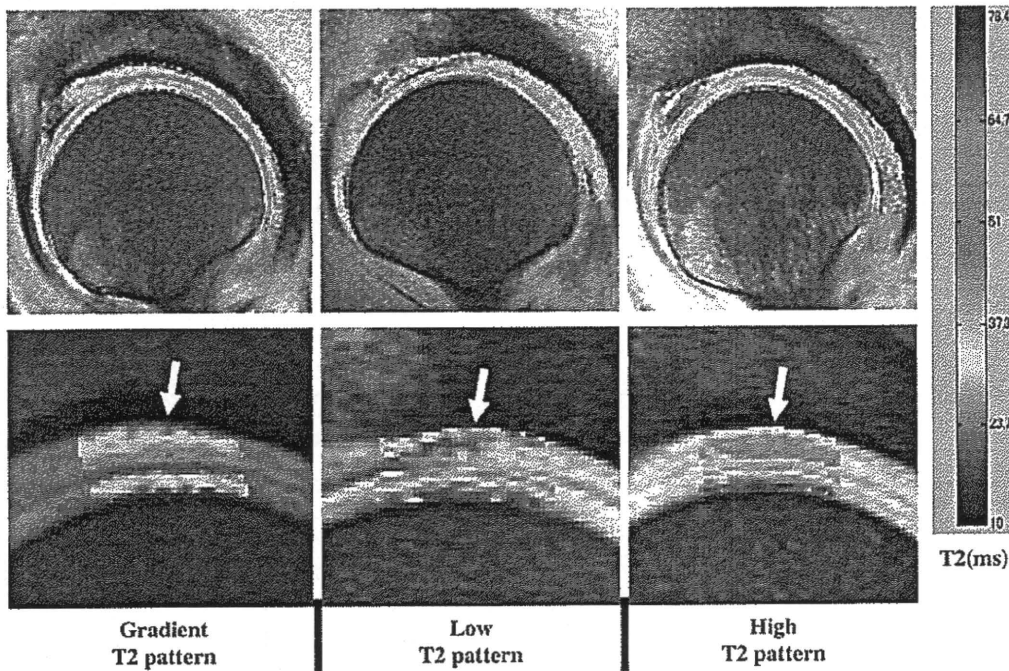


Fig. 2. Representative cases for the three patterns in visual appearance of T2 mapping (upper image) and their magnified images of the weight-bearing area with segmentation of the ROIs in the acetabular and femoral cartilages (lower image). Note T2 distribution within the ROIs of the acetabular cartilage (arrows). Gradient T2 pattern shows low T2 at the deep cartilage area and high T2 values at the superficial cartilage area; low T2 pattern shows predominantly low T2; and high T2 pattern shows predominantly high T2.

## Results

The average ages of the normal, pre-arthritic, and early-arthritic groups were 34 years (range, 23–51), 35 years (range, 22–50), and 45 years (range, 23–69), respectively. The mean height/weight of the three groups were 163 cm/54 kg, 156 cm/50 kg, and 157 cm/55 kg, respectively; there was no statistical difference of age and weight among the three groups, however, height of the normal group was significantly higher than the other two groups ( $P < 0.05$ ). All hips in the normal group, four hips in the pre-arthritic group, and two hips in the early-arthritic group showed no pain, while the other 10 hips in the pre-arthritic group and 10 hips in the early-arthritic group showed slight or relatively mild pain with WOMAC pain scores ranging from 1 to 12 points.

There was no significant difference in T2 value at the defined superior ROI of the cartilage among the normal, pre-arthritic, and early-arthritic groups, both for the acetabular and femoral sides. On the acetabular cartilage ROI, the mean T2 values  $\pm 1$  standard deviation for the normal, pre-arthritic, and early-arthritic groups were 33.4 ms  $\pm$  4.5, 32.0 ms  $\pm$  3.9, and 37.1 ms  $\pm$  12.0, respectively. On the femoral cartilage ROI, these values were 29.4 ms  $\pm$  3.0, 29.0 ms  $\pm$  4.4, and 28.0 ms  $\pm$  3.7, respectively.

The visual appearance of T2 mapping for the acetabular ROI showed a different distribution of the three patterns among the normal, pre-arthritic, and early-arthritic groups (Fig. 3). On the acetabular ROI, all hips in the normal group demonstrated gradient T2 pattern, while six hips in the pre-arthritic group (43%) and four hips in the early-arthritic group (33%) demonstrated low T2 pattern. The remaining eight hips in the early group (67%) demonstrated high T2 pattern. Consequently, the frequency of the gradient pattern was significantly different between the normal (100%) and pre-arthritic/early-arthritic groups (31%) ( $P < 0.0001$ ). On the femoral ROI, the frequency of the gradient pattern was also significantly different between the normal (93%) and pre-arthritic/early-arthritic groups (50%) ( $P < 0.05$ ).

Comparing the 20 asymptomatic hips and 20 symptomatic hips, frequency of gradient pattern in the acetabular/femoral cartilages was significantly lower in the symptomatic hips (35%/40%) than the asymptomatic hips (75%/90%) ( $P < 0.05$ ). However, there was no significant difference in T2 value between the asymptomatic and symptomatic hips, and there was no significant correlation between WOMAC pain scores and T2 values at the superior ROI of the cartilage.

## Discussion

Degeneration of the articular cartilage in osteoarthritis is associated with concomitant changes in the extracellular matrix components that include disruption of collagenous architecture, depletion of proteoglycan, or an increase/decrease in water content, even at very early stages of the disease<sup>30,31</sup>. There is a high expectation, based on numerous experimental and clinical studies, that assessment of T2 of the cartilage will become a potent surrogate of cartilage matrix changes such as these, as well as the associated loss of biomechanical function. Nieminen *et al.* observed an increase of T2 in the superficial zone of bovine cartilage following degradation of collagenous architecture by enzymatic treatment<sup>32</sup>. Lüsse *et al.* demonstrated a close correlation between the water content within the cartilage and T2 relaxation rates for human cartilage removed from the knee joint; the authors stated that the water content could be accurately estimated from the correlation of T2<sup>33</sup>. Wayne *et al.* showed significant inverse correlations of T2 with proteoglycan content or cartilage stiffness, using porcine patella cartilage with depletion of proteoglycan matrix following enzymatic treatment<sup>15</sup>. For *in vivo* imaging of the knee joint, an increase in T2 was associated with aging<sup>17,34</sup> and the involvement of osteoarthritis<sup>18</sup>, while a decrease in T2 was associated with the stress of running<sup>35</sup> and also with mechanical loading of the knee during MR imaging<sup>36</sup>. Other than the knee joint, T2 assessment *in vivo* has also been performed for interphalangeal joint cartilage<sup>37</sup>; however, to the best of our knowledge, T2 assessment of the hip joint has yet to be conducted.

Almost all hips of normal volunteers in the present study showed the gradient pattern of T2 mapping at the superior portion of the acetabular and femoral cartilages. This spatial variation, with T2 values increasing from the cartilage base toward the articular surface, is consistent with previous reports of normal knee cartilage T2 values *in vivo*<sup>17,28</sup>. This T2 distribution was accounted for histologically by the physiological spatial distribution of water, collagen and proteoglycan, and by spatial differences in collagenous architecture<sup>17</sup>. High T2 values in the limited distance from the bone/cartilage interface were described in a detailed quantitative analysis of T2 variation of normal knee cartilage<sup>17,28</sup>, but were not seen in the hip cartilages of the present study. T2 variations in these earlier studies of the knee were partly explained by chemical shift artifact and volume averaging artifact at the bone/cartilage interface<sup>17,28</sup>. Average T2 values of the acetabular and femoral cartilages in

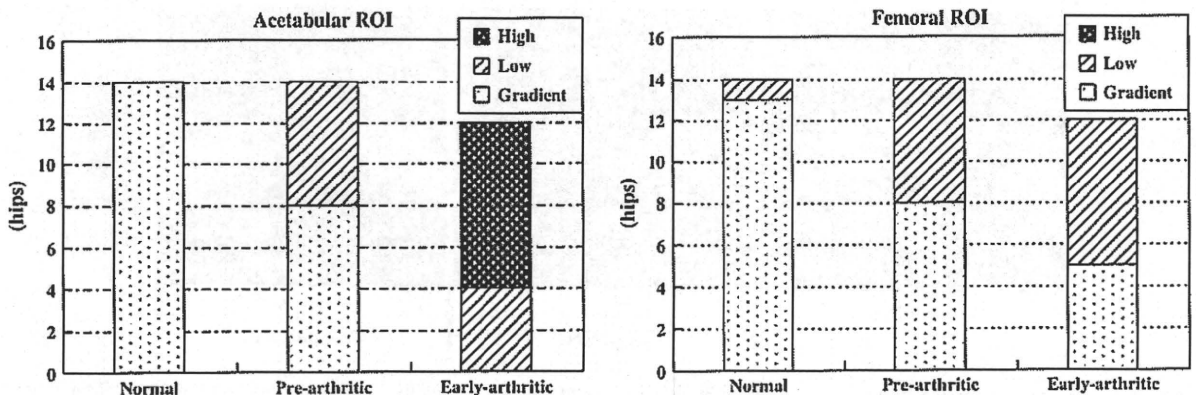


Fig. 3. Distribution of gradient T2 pattern, low T2 pattern and high T2 pattern in the normal, pre-arthritic, and early-arthritic groups, for the acetabular ROIs and femoral ROIs.

the healthy female volunteers (29–33 ms) of the present study were relatively low compared with those observed in the knee cartilages of healthy women of a similar age (40–60 ms) using 3 T MR imaging<sup>34</sup>. A previous cadaveric study revealed that mean cartilage thickness of the hip joint is significantly thinner than the thickness of cartilage in the knee joint, and that thinner cartilage is correlated with a higher compressive stiffness of the cartilage<sup>38</sup>. Considering that compressive stiffness of the cartilage is significantly related to water content or proteoglycan content<sup>39,40</sup>, the difference in average T2 values between our study and a previous knee study may partly reflect the physiological differences of those matrix components at the two sites.

The favorable results of the present study might partly result from the superior hardware capability of 3 T MR imaging. MR imaging of the hip cartilage has been difficult at conventional magnetic field strengths ( $\leq 1.5$  T) because of the relatively thin structure of the acetabular or femoral cartilages, their location deep inside the body, and the close contact between the acetabular and femoral cartilages<sup>41</sup>. MR imaging with high magnetic field strength improves image quality and precision because of the superior signal-to-noise ratio and spatial resolution<sup>19,42–44</sup>. If the cartilage thickness of the hip joints is generally assumed to range from 1 to 3 mm<sup>38,45</sup>, the MR images at 3 T in the present study contain approximately 3–10 pixels across each of the acetabular and femoral cartilages. We consider that this high-resolution imaging with high signal-to-noise ratio might be effective in classifying T2 mapping patterns and differentiating between the acetabular and femoral cartilages. However, additional studies to compare diagnostic accuracy and reproducibility between MR images at 3 T and at conventional 1.5 T are necessary to determine true advantages of using 3 T on imaging of hip cartilage.

In contrast to the normal hips of volunteers in the present study, the hips in the early-arthritic groups showed a high frequency of the high T2 pattern in the acetabular cartilage. The tendency of an increase in T2 associated with arthritic involvement agrees with previous results concerning high T2 in patients with knee osteoarthritis<sup>18</sup>. Abnormal elevation of T2 is accounted for pathologically by an increase in water content and water mobility associated with a decrease in proteoglycan content and disruption of the collagen network<sup>18,32</sup>. Predominant occurrence of high T2 pattern in the acetabular cartilage agrees with previous arthroscopic findings<sup>25</sup> showing high frequency of cartilage disorder in the superior acetabular cartilage at early-arthritic stages of hip dysplasia. An interesting finding of the present study is the high frequency of the low T2 pattern in the acetabular and femoral cartilage of the pre- and early-arthritic group. There are several possible explanations for this specific pattern of T2 mapping. First, the cartilage in dysplastic hips is prone to increasing biomechanical stress at the weight-bearing area due to reduced contact area between the opposing surfaces<sup>46</sup>. Previous interventional studies of the knee cartilage showed that axial loading by mechanical loading apparatus and cyclic compressive load by running exercise had a T2-shortening effect, presumably due to the loss of water content or an increase in collagen fiber anisotropy<sup>35,36</sup>. The long-term biomechanical environment of elevated stress distribution in dysplastic hips could lead to a different quantity and distribution of the cartilage matrix compared to normal hips, leading to different mapping of the low T2 pattern. Second, the articular cartilaginous structure of the hip progressively changes during postnatal developmental periods. In dysplastic hips, the inverted or hypertrophic labrum may cover the outer surface

of the acetabular articular cartilage after birth and may subsequently constitute a portion of the acetabular cartilage after the childhood developmental periods are completed<sup>47–49</sup>. Because the labrum has a considerably different extracellular matrix structure from the hyaline cartilage, with poor glycoaminoglycan and disorganized collagen fibrils<sup>49</sup>, acetabular cartilage with a mixture of original labral components might provide a low T2 pattern in T2 mapping. Hip of the early-arthritic group might present with either low T2 or high T2 pattern in the acetabular cartilage, depending on severity of involvement of degenerative changes. Although further follow-up of hips with high and low T2 patterns is needed to determine the clinical relevance of these specific patterns, it is tempting to suggest that T2 assessment may not only provide early detection of osteoarthritic degeneration but also enable the detection of developmental pathological disorders of the cartilage matrix that may lead to disorders of biomechanical function on load-bearing in cases of hip dysplasia.

Quantitative assessment of T2 values within the defined ROI failed to show significant differences among the three groups, although average T2 values of the acetabular ROI for the pre-arthritic group were relatively low and those for the early-arthritic group were relatively high, as compared with the normal group. There is considerable variation in T2 values along the cartilage depth in response to physiological non-uniform distribution of extracellular matrix in normal cartilage<sup>17,28</sup>. Degenerative change of matrix components in the early phase is likely to occur in a superficial or small localized area<sup>17</sup>. Average T2 values of bulk ROI from the cartilage base to the articular surface might be insufficiently sensitive to detect small T2 changes in a regional area, requiring the use of other quantitative methods such as comparison of T2 profile curves as a function of normalized distance from the bone/cartilage interface to the cartilage surface<sup>17,28</sup>, or the enhancement of abnormal T2 adjusted by standard T2 value distributions within the cartilage at each pixel.

Pain assessment using the WOMAC score was not correlated with T2 assessment in the hip cartilage at the superior zone. This absence of correlation may partly reflect the relatively mild level of hip pain in the present study. In addition, there are many potential sources of hip pain other than disorders of the articular cartilage, including labral tear, synovitis, ganglionic cyst, and loose body<sup>50</sup>. Previous arthroscopic studies for dysplastic hips at the pre-arthritic stage indicated a high correlation between hip pain and labral tear<sup>51</sup>. The status of labral disorders might have a stronger influence on pain severity than the status of articular cartilage disorders investigated in the present study.

There are several limitations in the present study. First, the pulse sequences available in this study meant that T2 values were calculated from two echoes. In many previous studies, T2 was calculated from more than two echo images and the initial echo image obtained from a multi-echo sequence was excluded in calculating T2 to minimize T2 inaccuracy caused by stimulated echoes<sup>17,28,37</sup>; however, a previous study that used a dual-echo spin-echo sequence for T2 assessment successfully achieved significant differences between the knee cartilages of healthy subjects and those of patients with osteoarthritis<sup>18</sup>. Given the similarities of the gradient pattern of T2 mapping in the present study to previous findings in knee cartilage<sup>17,28</sup>, we consider that T2 assessment using a dual-echo spin-echo sequence allowed reliable assessment of the extracellular matrix in the hip cartilage. Second, reliability of T2 assessment was influenced both by reproducibility of acquisition of

MR images and reproducibility of T2 calculation such as definition of ROI or judgment of visual appearance of T2 mapping patterns. Acceptable reproducibility of T2 calculation was obtained in this study with inter-observer reliability ranging from 2.5% to 3.8%. However, reproducibility of acquisition of MR images by scanning repeatedly was not evaluated, and it is unknown how variations in acquisition of MR images influenced the outcomes. Third, this was a feasibility study that conducted comparison of T2 values and mapping patterns between the normal hips and dysplastic hips only at the superior zone, where assessment is particularly important for dysplastic hips, based on biomechanical condition and assessment of osteoarthritis progression. However, additional care should be taken in interpreting T2 values in further studies to assess other anterior or posterior areas of the hip cartilage. Collagen fibril orientation of the cartilage against the static magnetic field differs considerably between the anterior, superior, and posterior regions because of the strongly curved structure of the articular cartilage of the hip. Assessment of T2 values may be significantly influenced by the variations in collagen fibril orientation associated with cartilage positions<sup>52</sup>. Finally, the number of normal volunteers and patients with hip dysplasia was small. The subjects were limited to female gender, and predominantly young subjects were examined both in volunteers and patients, partly due to the low frequency of pre-arthritic or early-arthritic stages in older patients with hip dysplasia. Previous reports showed that T2 in the knee joint was influenced significantly by age<sup>17</sup> and insignificantly by gender<sup>21</sup>; however, it is unknown whether these factors influence the T2 of hip cartilage. Further studies are required to explore the degree of influence of age, gender, and other relevant factors on hip cartilage T2.

In summary, this preliminary study reveals that T2 assessment using 3 T MR imaging shows promise in the early detection of osteoarthritic degeneration and in the detection of developmental pathological disorders of cartilage matrix in patients with hip dysplasia. A combination of T2 assessment and other quantitative assessment techniques such as dGEMRIC<sup>53</sup>, which is sensitive to cartilage proteoglycan content, may enable further detailed assessment of fundamental cartilage disorders in patients with dysplastic hips and enhance the early detection of the degeneration of hip cartilage.

#### Acknowledgments

This work was partly supported by Grant-in-Aid for Scientific Research, the Ministry of Education, Science and Culture in Japan, and Grant of Japan Hip Research Foundation, Inc.

#### References

- Harris WM. Etiology of osteoarthritis of the hip. *Clin Orthop* 1986;213:20–33.
- Nakamura S, Ninomiya S, Nakamura T. Primary osteoarthritis of the hip joint in Japan. *Clin Orthop* 1989;241:190–6.
- Lane NE, Lin P, Christiansen L, Gore R, Williams EN, Hochberg MC, *et al.* Association of mild acetabular dysplasia with an increased risk of incident hip osteoarthritis in elderly white women: the study of osteoporotic fractures. *Arthritis Rheum* 2000;43:400–4.
- Hasegawa Y, Iwata H, Mizuno M, Genda E, Sato S, Miura T. The natural course of osteoarthritis of the hip due to subluxation or acetabular dysplasia. *Arch Orthop Trauma Surg* 1992;111:187–91.
- Anwar MM, Sugano N, Matsui M, Takaoka K, Ono K. Dome osteotomy of the pelvis for osteoarthritis secondary to hip dysplasia: an over five-year follow-up study. *J Bone Joint Surg Br* 1993;75-B:222–7.
- McCrae F, Shouls J, Dieppe P, Watt I. Scintigraphic assessment of osteoarthritis of the knee joint. *Ann Rheum Dis* 1992;51:938–42.
- Nishii T, Tanaka H, Nakanishi K, Sugano N, Miki H, Yoshikawa H. Fat-suppressed 3D spoiled gradient-echo MRI and MDCT arthrography of articular cartilage in patients with hip dysplasia. *AJR Am J Roentgenol* 2005;185:379–85.
- Nishii T, Sugano N, Sato Y, Tanaka H, Miki H, Yoshikawa H. Three-dimensional distribution of acetabular cartilage thickness in patients with hip dysplasia: a fully automated computational analysis of MR imaging. *Osteoarthritis Cartilage* 2004;12:650–7.
- Schmid MR, Nötzli HP, Zanetti M, Wyss TF, Hodler J. Cartilage lesions in the hip: diagnostic effectiveness of MR arthrography. *Radiology* 2003;226:382–6.
- Zhai G, Cicuttini F, Srikanth V, Cooley H, Ding C, Jones G. Factors associated with hip cartilage volume measured by magnetic resonance imaging: the Tasmanian Older Adult Cohort Study. *Arthritis Rheum* 2005;52:1069–76.
- Fife RS, Brandt KD, Braunstein EM, Katz BP, Shelbourne KD, Kalasinski LA, *et al.* Relationship between arthroscopic evidence of cartilage damage and radiographic evidence of joint space narrowing in early osteoarthritis of the knee. *Arthritis Rheum* 1991;34:377–82.
- Felson DT. The course of osteoarthritis and factors that affect it. *Rheum Dis Clin North Am* 1993;19:607–15.
- Buckwalter JA, Mankin HJ. Articular cartilage: degeneration and osteoarthritis, repair, regeneration, and transplantation. *Instr Course Lect* 1998;47:487–504.
- Burstein D, Gray ML. Is MRI fulfilling its promise for molecular imaging of cartilage in arthritis? *Osteoarthritis Cartilage* 2006;14:1087–90.
- Wayne JS, Kraft KA, Shields KJ, Yin C, Owen JR, Disler DG. MR imaging of normal and matrix-depleted cartilage: correlation with biomechanical function and biochemical composition. *Radiology* 2003;228:493–9.
- Liess C, Lüsse S, Karger N, Heller M, Glüer CC. Detection of changes in cartilage water content using MRI T2-mapping *in vivo*. *Osteoarthritis Cartilage* 2002;10:907–13.
- Mosher TJ, Dardzinski BJ, Smith MB. Human articular cartilage: influence of aging and early symptomatic degeneration on the spatial variation of T2- preliminary findings at 3T. *Radiology* 2000;214:259–66.
- Dunn TC, Lu Y, Jin H, Ries MD, Majumdar S. T2 relaxation time of cartilage at MR imaging: comparison with severity of knee osteoarthritis. *Radiology* 2004;232:592–8.
- Gold GE, Suh B, Sawyer-Glover A, Beaulieu C. Musculoskeletal MRI at 3.0 T: initial clinical experience. *AJR Am J Roentgenol* 2004;183:1479–86.
- Inoue K, Wichart P, Kawasaki T, Huang J, Ushiyama T, Hukuda S, *et al.* Prevalence of hip osteoarthritis and acetabular dysplasia in French and Japanese adults. *Rheumatology (Oxford)* 2000;39:745–8.

21. Mosher TJ, Collins CM, Smith HE, Moser LE, Sivarajah RT, Dardzinski BJ, *et al.* Effect of gender on *in vivo* cartilage magnetic resonance imaging T2 mapping. *J Magn Reson Imaging* 2004;19:323-8.
22. Fredensborg N. The CE angle of normal hips. *Acta Orthop Scand* 1976;47:403-5.
23. Crowe JF, Mani VJ, Ranawat CS. Total hip replacement in congenital dislocation and dysplasia of the hip. *J Bone Joint Surg Am* 1979;61-A:15-23.
24. Kellgren JH, Lawrence JS. Radiological assessment of osteo-arthritis. *Ann Rheum Dis* 1957;16:494-502.
25. Noguchi Y, Miura H, Takasugi S, Iwamoto Y. Cartilage and labrum degeneration in the dysplastic hip generally originates in the anterosuperior weight-bearing area: an arthroscopic observation. *Arthroscopy* 1999;15:496-506.
26. Maier CF, Tan SG, Hariharan H, Potter HG. T2 quantitation of articular cartilage at 1.5 T. *J Magn Reson Imaging* 2003;17:358-64.
27. Yao L, Gentili A, Thomas A. Incidental magnetization transfer contrast in fast spin-echo imaging of cartilage. *J Magn Reson Imaging* 1996;6:180-4.
28. Smith HE, Mosher TJ, Dardzinski BJ, Collins BG, Collins CM, Yang QX, *et al.* Spatial variation in cartilage T2 of the knee. *J Magn Reson Imaging* 2001;14:50-5.
29. Bellamy N, Buchanan WW, Goldsmith CH, Campbell J, Stitt LW. Validation study of WOMAC: a health status instrument for measuring clinically important patient relevant outcomes to antirheumatic drug therapy in patients with osteoarthritis of the hip or knee. *J Rheumatol* 1988;15:1833-40.
30. Mankin HJ, Dorfman H, Lippicello L, Zarins A. Biochemical and metabolic abnormalities in articular cartilage from osteo-arthritic human hips. II. Correlation of morphology with biochemical and metabolic data. *J Bone Joint Surg Am* 1971;53-A:523-37.
31. Panula HE, Hyttinen MM, Arokoski JP, Langsjö TK, Peltari A, Kiviranta I, *et al.* Articular cartilage superficial zone collagen birefringence reduced and cartilage thickness increased before surface fibrillation in experimental osteoarthritis. *Ann Rheum Dis* 1998;57:237-45.
32. Nieminen MT, Töyräs J, Rieppo J, Hakumäki JM, Silvennoinen J, Helminen HJ, *et al.* Quantitative MR microscopy of enzymatically degraded articular cartilage. *Magn Reson Med* 2000;43:676-81.
33. Lüsse S, Claassen H, Gehrke T, Hassenpflug J, Schunke M, Heller M, *et al.* Evaluation of water content by spatially resolved transverse relaxation times of human articular cartilage. *Magn Reson Imaging* 2000;18:423-30.
34. Mosher TJ, Liu Y, Yang QX, Yao J, Smith R, Dardzinski BJ, *et al.* Age dependency of cartilage magnetic resonance imaging T2 relaxation times in asymptomatic women. *Arthritis Rheum* 2004;50:2820-8.
35. Mosher TJ, Smith HE, Collins C, Liu Y, Hancy J, Dardzinski BJ, *et al.* Change in knee cartilage T2 at MR imaging after running: a feasibility study. *Radiology* 2005;234:245-9.
36. Nag D, Liney GP, Gillespie P, Sherman KP. Quantification of T<sub>2</sub> relaxation changes in articular cartilage with *in situ* mechanical loading of the knee. *J Magn Reson Imaging* 2004;19:317-22.
37. Lazovic-Stojkovic J, Mosher TJ, Smith HE, Yang QX, Dardzinski BJ, Smith MB. Interphalangeal joint cartilage: high-spatial-resolution *in vivo* MR T2 mapping - a feasibility study. *Radiology* 2004;233:292-6.
38. Shepherd DE, Seedhom BB. Thickness of human articular cartilage in joints of the lower limb. *Ann Rheum Dis* 1999;58:27-34.
39. Armstrong CG, Mow VC. Variations in the intrinsic mechanical properties of human articular cartilage with age, degeneration, and water content. *J Bone Joint Surg Am* 1982;64-A:88-94.
40. Kempson GE, Muir H, Swanson SA, Freeman MA. Correlations between stiffness and the chemical constituents of cartilage on the human femoral head. *Biochim Biophys Acta* 1970;215:70-7.
41. Hayes CW, Balkissoon AA. Magnetic resonance imaging of the musculoskeletal system. II. The hip. *Clin Orthop* 1996;322:297-309.
42. Gold GE, Han E, Stainsby J, Wright G, Brittain J, Beaulieu C. Musculoskeletal MRI at 3.0 T: relaxation times and image contrast. *AJR Am J Roentgenol* 2004;183:343-51.
43. Eckstein F, Charles HC, Buck RJ, Kraus VB, Remmers AE, Hudelmaier M, *et al.* Accuracy and precision of quantitative assessment of cartilage morphology by magnetic resonance imaging at 3.0T. *Arthritis Rheum* 2005;52:3132-6.
44. Fischbach F, Bruhn H, Unterhauser F, Rieke J, Wieners G, Felix R, *et al.* Magnetic resonance imaging of hyaline cartilage defects at 1.5T and 3.0T: comparison of medium T2-weighted fast spin echo, T1-weighted two-dimensional and three-dimensional gradient echo pulse sequences. *Acta Radiol* 2005;46:67-73.
45. Kurrat HJ, Oberländer W. The thickness of the cartilage in the hip joint. *J Anat* 1978;126:145-55.
46. Hipp JA, Sugano N, Millis MB, Murphy SB. Planning acetabular redirection osteotomies based on joint contact pressure. *Clin Orthop* 1999;364:134-43.
47. Tachdjian MO. Congenital dysplasia of the hip. In: Wickland Jr EH, Ed. *Pediatric Orthopedics*. Philadelphia: Saunders WB 1990;Volume 1:297-312.
48. Dunn PM. Perinatal observations on the etiology of congenital dislocation of the hip. *Clin Orthop* 1976;119:11-22.
49. Ponseti IV. Morphology of the acetabulum in congenital dislocation of the hip. Gross, histological and roentgenographic studies. *J Bone Joint Surg Am* 1978;60-A:586-99.
50. Baber YF, Robinson AH, Villar RN. Is diagnostic arthroscopy of the hip worthwhile? A prospective review of 328 adults investigated for hip pain. *J Bone Joint Surg Br* 1999;81-B:600-3.
51. Suenaga E, Noguchi Y, Jingushi S, Shuto T, Nakashima Y, Miyanishi K, *et al.* Relationship between the maximum flexion-internal rotation test and the torn acetabular labrum of a dysplastic hip. *J Orthop Sci* 2002;7:26-32.
52. Xia Y. Magic-angle effect in magnetic resonance imaging of articular cartilage: a review. *Invest Radiol* 2000;35:602-21.
53. Kim YJ, Jaramillo D, Millis MB, Gray ML, Burstein D. Assessment of early osteoarthritis in hip dysplasia with delayed gadolinium-enhanced magnetic resonance imaging of cartilage. *J Bone Joint Surg Am* 2003;85-A:1987-92.

シンポジウム

変形性膝関節症のマネジメント —最新の臨床エビデンスとエキスパートオピニオン—

### 変形性膝関節症の手術療法\*

松本 秀男†

#### はじめに

変形性膝関節症(OA)は要約すれば膝関節の老化であり、近年の高齢化社会に伴い、その患者数は著しく増加している<sup>1)</sup>(図1, 2)。本疾患自体は重篤な全身症状を来すものではないが、疼痛のために日常生活動作が著しく制限され、さらにそれに伴って全身的にも多くの障害を併発する。軽症例に対してはさまざまな保存的治療が行われているが、基本的にOAの完治を目指すものではなく、症状の軽減を図るものがほとんどである。OAが進行すると、保存的治療では対処できないこともあり、その際には手術療法が適応となる。手術法としては joint débridement (関節デブリドマン)、高位胫骨骨切り術、人工膝関節置換術が主なものである。本稿ではこれらの現在一般に行われているOAに対する手術療法を紹介する。

#### 1. Joint débridement (関節デブリドマン)

OAに伴う関節軟骨の破片などの関節内遊離体の除去、損傷半月板の切除、増殖した滑膜の切除などを行う方法であり、通常関節鏡を用いて行う(図3)。また、関節鏡視下に関節軟骨に傷をつけて、その再生を促すマイクロフラクチャーやドリリング、さらには伸展制限を軽減することを目的とする後方解離術などを追加する方法も行われている<sup>2),3)</sup>。

#### 1) 適応

本手術法はOAを根本的に治す手術ではなく、OA

に伴って剝離した軟骨の除去や、損傷した半月板の処置などを行う対症的な手術であることを念頭に置く必要がある。したがって、手術適応は比較的軽度のOAで、半月板や遊離軟骨片がロッキングするなどの機械的な因子によるものが主症状であり、関節鏡視下にこれら

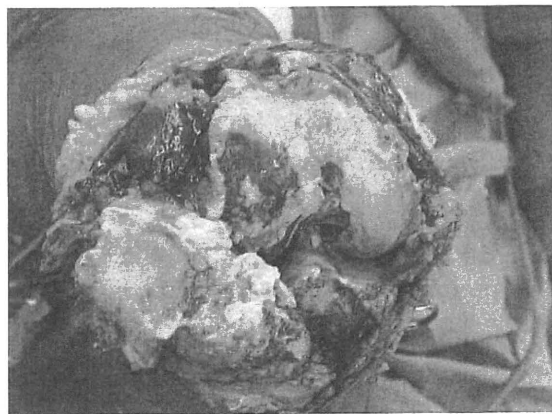


図1 変形性膝関節症の肉眼所見。関節軟骨の荒廃と著しい骨棘形成を認める。



図2 変形性膝関節症の単純X所見。胫骨内側顆の陥凹、内側関節裂隙の狭小化、骨棘形成を認める。

**Key words:** Osteoarthritis, Knee Joint, Joint débridement, High tibial osteotomy, Total knee arthroplasty

\*Operative treatment for osteoarthritis of the knee joint  
†慶應義塾大学スポーツ医学総合センター。Hideo Matsumoto: Institute for Integrated Sports Medicine, Keio University

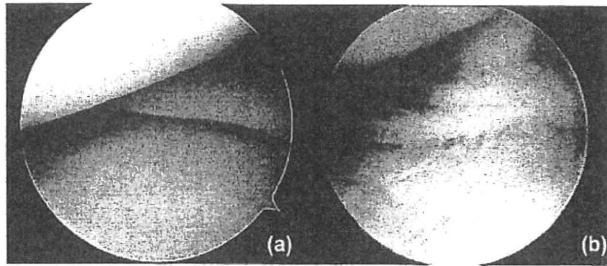


図3 正常膝関節(a)と変形性膝関節症(b)の関節鏡所見。変形性膝関節症では半月板や関節軟骨の変性を認める。

を除去することにより、症状の改善が得られると判断できる場合がよい適応である。OAに伴う滑膜増殖により関節水症が続く症例に対して、関節鏡視下滑膜切除を中心に本手術法が行われることもあるが、変形性変化は残存するため、その効果は限定的である。

### 2) 術前チェック

病歴、診察所見から安静時痛や夜間痛などが主症状でなく、関節運動時の疼痛など機械的な要素が主であることを確認する。術前に単純X線だけでなく、MRI (magnetic resonance imaging) 等で関節軟骨、半月板、滑膜などの関節構成体の状態を把握し、機械的因子が現在の症状の主原因であることを確認する。

### 3) 手術方法

通常内側および外側傍膝蓋ポータルより鏡視を行う。まず関節鏡視下に関節構成体の状態を確認する。損傷半月や関節軟骨などが関節内遊離体になっている

場合はこれを摘出する。半月板は変性していることが多いが、関節運動に影響する機械的因子になっていない場合は、通常放置する。関節軟骨の部分的剝離を認めることも多いが、これも機械的因子になっていない場合は放置する。滑膜切除を行う場合には電動シェーバーが有用であるが、内外側の谷部や後方の滑膜切除は通常のポータルから行うことは難しいので、必要な場合にはポータルを追加する。マイクロフラクチャーやドリリング、後方解離術などを行う場合はこれを追加するが、本稿では詳細は省略する。

## 2. 高位脛骨骨切り術

### (high tibial osteotomy, HTO)

内反型のOAに対して脛骨中枢部で骨切りを行って下肢全体の軸を外反し、膝関節内側部に加わる荷重を減少することにより、症状の軽減を図るものである(図4)。本法により術後荷重が軽減された膝関節内側部の軟骨の修復が得られたとする報告もある。

#### 1) 適応

内側コンパートメントの変化を中心とした内反型のOAで、外側コンパートメントや膝蓋大腿関節の変形性変化が強くないものがよい適応である。著しい伸展制限や膝蓋骨低位のある症例は適応が制限される。術後関節軟骨の修復が得られたとする報告はあるものの、荷重条件を変えることが主な目的であり、病変部には手術操作を加えないためOAの根本的な治療ではない。後に述べる人工関節置換術に比べ生物学的な治療であり、年齢が低く人工関節を適応しにくい症例



図4 高位脛骨骨切り術(closed wedge osteotomy)。脛骨中枢部で外側を底辺とする三角形の骨片を切除して外反を図る。

に対しても適応されることがある。また、関節内に機械的な疼痛要因が合併する場合には joint débridement を併用することもある。

## 2) 術前チェック

病歴、診察所見から内側部に主症状があることを確認する。術前に単純 X 線は通常の 3 方向だけでなく、下肢荷重時(立位)正面像を撮影し、荷重時の膝関節内反変形の程度を定量化して、骨切り角度を計画しておく。通常は荷重時の外反角(FTA, femoro-tibial angle)を計測する。正常下肢の FTA は 173°前後であるが、荷重をより外側に変位させることと、術後の再内反の可能性を考慮して、FTA: 167-8°程度を骨切り目標角度とすることが多い。また、可能であれば MRI 等で関節軟骨、半月板、滑膜などの関節構成体の状態も把握しておく。

## 3) 手術方法

外側部を底辺とする三角形の骨片を切除して外反を図る closed wedge osteotomy と水平に骨切りを行った後、内側部を底辺とする三角形の骨片または人工骨を移植して外反を図る open wedge osteotomy, 正面からみてドーム形に骨切りを行い、脛骨末梢部を回転させる dome osteotomy がある<sup>4),5)</sup>。また、脛骨を骨切りするにあたって、腓骨の骨切りも同時に要するが、これも腓骨の中央部で骨切りする方法、中枢 1/3 で骨切りする方法、近位脛腓関節をはずす方法などがある。

Closed wedge osteotomy および open wedge osteotomy は手技的には比較的容易であり、外反角のコントロールもしやすいことが長所である。しかし、closed wedge osteotomy では、膝関節外側部の緩みが生じること、膝蓋骨高位になりやすいこと、骨切り面の外側部の形状が合いにくいいため、固定が難しく、脛骨の末梢部が中枢部にめり込んで過外反になりやすい、などの欠点がある。Open wedge osteotomy では、腓骨の骨切りを要さない長所がある反面、大きな矯正は難しいこと、膝関節内側部が過緊張になりやすいこと、膝蓋骨低位になりやすいこと、自家骨を移植する場合には骨採取を要することなどが欠点である。一方、dome osteotomy は骨切りを行った後、術中に外反角度を調整できる長所があるが、手術手技が比較的難しいこと、固定に創外固定を要することが多いことなどが欠点である。

腓骨の骨切り部位は遠位で行うほど、合併症で問題となる腓骨神経損傷が生じにくくなるが、脛骨の骨切り部位と離れると骨切り部の先端の移動距離が大きくなる。また、通常腓骨が早期に再癒合して、脛骨の骨癒合を障害することを防止するため、ある程度の長さを切除することが多い。

## 3. 人工膝関節置換術

OA により荒廃した関節面を切除して、人工物で置き換える手術である。膝関節の内側または外側コンパートメントのいずれか一方だけを置換する単顆置換術(unicompartmental knee arthroplasty, UKA, 図 5)



図 5 単顆置換術(UKA)術後の単純 X 線所見。膝関節の内側コンパートメントだけを置換する。





図6 全人工膝関節置換術(TKA)後の肉眼所見. 荒廃した大腿骨, 胫骨, 膝蓋骨関節面を切除しインプラントに置換する.

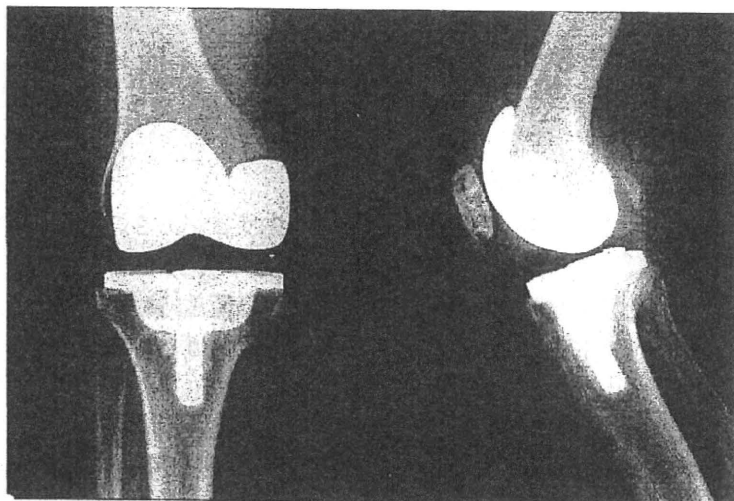


図7 全人工膝関節置換術(TKA)後の単純X線所見. 大腿骨, 胫骨, 膝蓋骨すべての関節面がインプラントに置換されている.

と両方のコンパートメントと膝蓋大腿関節のすべてを置換する全置換術(total knee arthroplasty, TKA, 図6, 7)がある<sup>6),7)</sup>. 大腿骨関節面は金属, 胫骨と膝蓋骨関節面は高分子ポリエチレンで置き換えるものが多いが, セラミックなどの素材も開発されている. OAによる病変部そのものを置換するため, 除痛効果に優れるが, 高齢者にとっては侵襲の大きな手術であり, また感染, 長期的に人工関節の緩みなどの合併症に十分な注意が必要である.

### 1) 適応

OAによる関節面の荒廃が著しく, 保存療法や他の手術では十分な効果が得られない場合に選択する. 高度の内外反変形や回旋変形, 著しい骨欠損, 可動域制限の強い例などに対しても, ささまざまなオプションの関節や充填用のブロックなどが開発されている. 長期的な人工関節の緩みが問題となるので, 年齢が低い場合には適応を慎重に決定する. また侵襲の大きな手術であり, 全身的にさまざまな合併症を持つ人に対しては慎重に適応を検討する. UKAは明らかに内側または外側コンパートメントのいずれか一方だけの変化が強い場合に適応する. 大腿骨顆部の骨壊死後に生じたOAなどは他のコンパートメントの変化が軽い場合が多く, 良い適応である.

### 2) 術前チェック

病歴, 診察所見から膝関節痛による日常生活動作の

障害程度を確認する. 単純X線は下肢荷重時(立位)正面像も撮影し, 内側関節裂隙の狭小化の程度, 胫骨内側関節面の損傷程度を定量化し, 大腿骨および胫骨の骨切り角度を計画しておく. また著しい骨欠損や変形を認める症例では, 骨欠損の充填用ブロックや固定用延長ステムなどを術前に計画して用意しておく.

### 3) 手術方法

通常, 傍膝蓋内側皮膚切開で進入する. それぞれの人工関節に専用の骨切りガイドが開発されており, これを用いて術前に計画した通りに大腿骨と胫骨関節面の骨切りを進める. 膝蓋骨は置換する方法としない方法があり, 置換する場合には骨切りを行い, しない場合には骨棘の切除等を行う. 正確な骨切りが完了し, 軟部組織のバランスが取れたら, インプラントを挿入する. インプラントの固定は骨セメントを用いる場合と, プレスフィット, すなわち直接固定する方法がある. また, 近年, ナビゲーションシステムを用いて, より正確に骨切りを行う試み(図8)や, 皮膚切開や大腿四頭筋への侵襲をできるだけ小さく手術を行う最小侵襲人工膝関節置換術(minimally invasive surgery-TKA, MIS-TKA, 図9)<sup>8),9)</sup>が開発され, 臨床応用されている.

### おわりに

変形性膝関節症は進行すると日常生活でも疼痛を伴うようになる. 疼痛を伴う生活はきわめて苦痛であ



図8 ナビゲーションを用いた膝関節置換術(膝関節置換術(全人工TKA)). 骨切りガイドと骨との間の角度を定量的に表示できる.

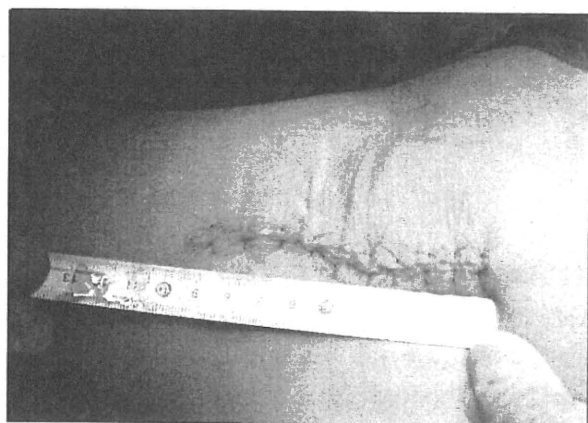


図9 最小侵襲人工膝関節置換術(MIS-TKA)の皮膚切開. 7-10 cm程度の皮膚切開で手術が可能である.

り, 解決できるのであれば, 解決すべきである. しかし, 手術療法はさまざまなリスクも伴うため, 手術によるメリットとデメリットを慎重に吟味して適応を決めることが大切である.

### 文 献

1) 戸山芳昭, 中村耕三, 越智光夫他. 変形性膝関節症に対する手術療法: 過去10年における手術法選択の推移 —日本整形外科学会認定研修施設を対象と

した全国アンケート集計結果—. 日整会誌 2007; 81: 585-9.  
 2) Yen YM, Cascio B, O'Brien L, et al. Treatment of osteoarthritis of the knee with microfracture and rehabilitation. Med Sci Sports Exerc 2008; 40: 200-5.  
 3) Moriya H, Sasho T, Sano S, et al. Arthroscopic posteromedial release for osteoarthritic knees with flexion contracture. Arthroscopy 2004; 20: 1030-9.  
 4) 齋藤知行, 腰野富久. 横浜市大式高位胫骨骨切り術. HTO. 新 OS NOW. 24 膝関節外科 —手術手技のすべて. 岩本幸英他編. 東京: Medical View社; 2004. p.76-82.  
 5) 井原秀俊. ドーム式. HTO. 新 OS NOW. 24 膝関節外科 —手術手技のすべて. 岩本幸英他編. 東京: Medical View社; 2004. p.64-8.  
 6) 秋月章. 最小侵襲人工膝単顆置換術. TKA. 新 OS NOW. 24 膝関節外科 —手術手技のすべて. 岩本幸英他編. 東京: Medical View社; 2004. p.121-7.  
 7) 松野誠夫, 龍順之助, 勝呂徹他. 人工膝関節置換術—基礎と臨床—. 東京: 文光堂; 2005.  
 8) 須田康文, 松本秀男, 大谷俊郎他. 人工膝関節全置換術に対するナビゲーションシステムの応用. 膝 2003; 28: 76-9.  
 9) 松本秀男, 大谷俊郎, 松崎健一郎他. 大腿四頭筋温存型人工膝関節—手術技法と問題点. 整形外科 2006; 57: 84-8.

## Case Report

# Double-Concave Deformity of the Polyethylene Tibial Post in Posterior Stabilized Total Knee Arthroplasty

Yasuo Niki, MD,\* Hideo Matsumoto, MD,\* Fumihiro Yoshimine, MD,†  
Yoshiaki Toyama, MD,\* Yasunori Suda, MD,\* and Scott A. Banks, PhD‡

**Abstract:** This report describes a unique case of bilateral total knee arthroplasty necessitating revision of the polyethylene insert, which showed prominent marks on the tibial post resulting from repeated *seiza*-style sitting. The patient presented 7 years postoperatively with knee pain and flexion disturbance due to continuous joint effusion persisting for more than 4 months. Proliferating synovia throughout the joint revealed reactive synovitis to polyethylene particles. The retrieved polyethylene inserts displayed double-concave deformity of the tibial post with burnishing and creep in tibiofemoral articulation. The damage pattern of retrieved polyethylene inserts reflected the data from tibiofemoral contact location obtained using a shape-matching technique in the early postoperative phase. This case provides an example of damage to the polyethylene tibial post caused by a floor-sitting lifestyle and the potential clinical sequelae.  
**Keywords:** total knee arthroplasty, deep flexion, polyethylene insert, tibial post, floor-sitting lifestyle, shape matching.

© 2010 Elsevier Inc. All rights reserved.

With increasing progress in surgical techniques, implant design, and biomaterials, the ability to achieve greater than 145° of deep flexion is increasingly requested by patients undergoing total knee arthroplasty (TKA), particularly in Asian and Middle Eastern countries. In the late 1990s, several manufacturers developed implants with a high-flex knee design; however, the safety of very deep flexion and the effects of this activity on implant longevity remain unclear. Herein, we report the case of a 69-year-old man for whom Japanese *seiza*-style sitting was an important activity of daily living after bilateral TKA. At 7 years postoperatively, the patient presented with persistent joint effusion of both knees, for which revision of the polyethylene inserts alone resulted in complete recov-

ery. In fact, knee kinematics of the patient during *seiza*-style sitting had been analyzed in the early postoperative phase using model-based shape-matching techniques. The damage pattern of retrieved polyethylene inserts reflected these shape-matching data, providing valuable information on the long-term effects of *seiza*-style sitting.

### Case Report

A 63-year-old man underwent bilateral primary TKA with the Stryker Scorpio posterior-stabilized knee system (Stryker Orthopaedics, Mahwah, NJ) in 2000. He recovered without any complications and returned to his original floor-sitting lifestyle, often participating in the tea ceremony, which requires knee flexion greater than 145°. At 3 months postoperatively, routine bilateral radiographs were obtained with the patient in the *seiza* (Japanese-style) sitting posture. Tibiofemoral orientation and contact/separation of the articular surfaces were determined using model-based shape-matching techniques, as previously reported [1]. Briefly, fluoroscopic images were digitized and corrected for static optical distortion. The implant surface model was projected onto the geometry-corrected image, and the 3-dimensional pose was adjusted to match the silhouette of the model to that of the TKA implants in the subject. The results of shape-matching analysis revealed

From the \*Department of Orthopaedic Surgery, Keio University, Shinjuku-ku, Tokyo, Japan; †Department of Orthopaedic Surgery, Tokyo Metropolitan Ohkubo Hospital, Tokyo, Japan; and ‡Department of Mechanical and Aerospace Engineering, University of Florida, Gainesville, Florida.

Submitted May 10, 2008; accepted February 8, 2009.

No benefits or funds were received in support of the study.

Reprint requests: Yasuo Niki, MD, PhD, Department of Orthopaedic Surgery, Keio University, 35, Shinanomachi, Shinjuku, Tokyo 160-8582, Japan.

© 2010 Elsevier Inc. All rights reserved.

0883-5403/09/2503-0029\$36.00/0

doi:10.1016/j.arth.2009.02.012

subtle articular surface separation occurring in the lateral tibiofemoral articulation of both knees, whereas cam/post and medial tibiofemoral articulation showed substantial contact in both knees (Fig. 1). Internal rotation of the tibia during *seiza*-style sitting was 9.5° for the right knee and 13.8° for the left knee, indicating minimum risk of posterior condylar subluxation. Seven years postoperatively, the patient presented with bilateral knee joint effusion, limiting deep flexion of the knees and disturbing his lifestyle. Laboratory testing showed negative results for inflammatory markers suggestive of deep infection, such as C-reactive protein or erythrocyte sedimentation rate, although aspiration of clear yellowish joint fluid indicated a paucity of active inflammatory cells migrating into the joint. According to radiography, metal components were well positioned with no signs of osteolysis or loosening; but joint spaces appeared slightly narrowed, suggesting polyethylene insert wear or creep (Fig. 2).

Joint effusion persisted for 4 months and was considered to be caused by reactive synovitis to wear particles from polyethylene. As metal components were well positioned, only the polyethylene inserts were revised to thicker inserts, bilaterally. Intraoperatively, synovial tissues proliferating throughout the joints were extensively excised. Pathologic findings revealed polyethylene particles surrounded by foreign body giant cells in places in synovia with villous phenotype (Fig. 3). Both retrieved inserts displayed burnishing and dimensional changes (Fig. 4A), which have been reported in 30% of retrievals of this type [2]. The

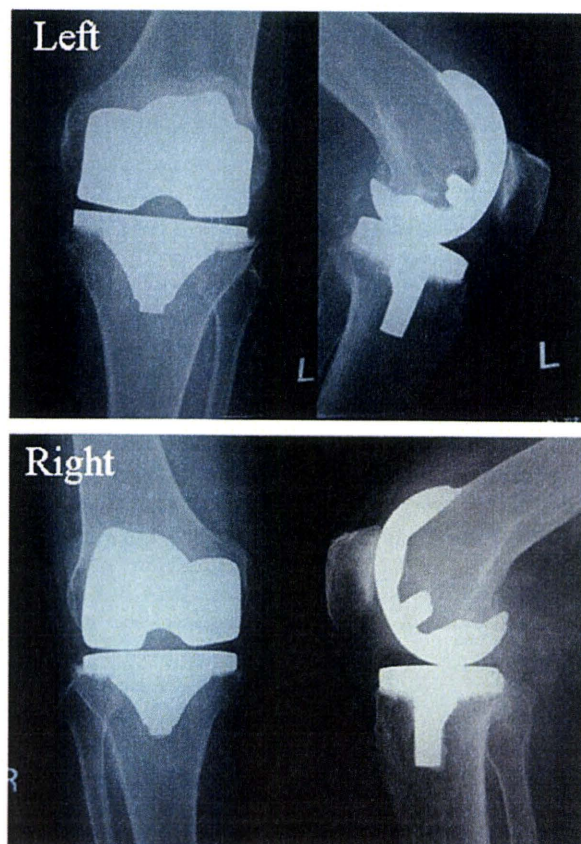


Fig. 2. Radiographs at 7 years postoperatively, suggesting polyethylene insert wear or creep.

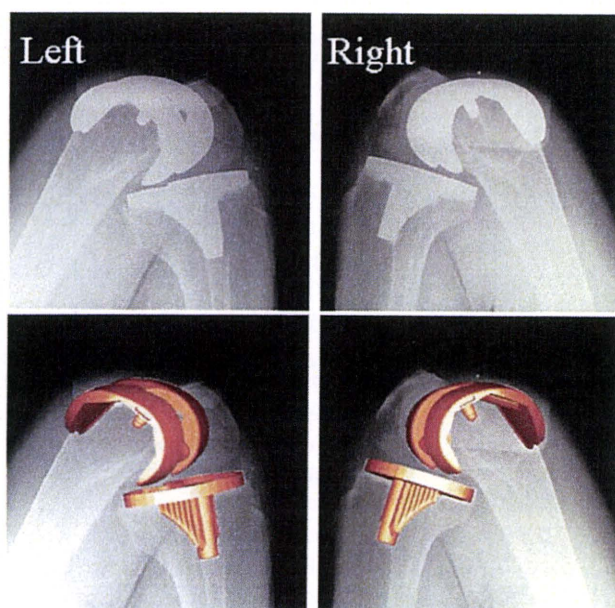


Fig. 1. Shape-matching data of *seiza*-style sitting 3 months after TKA. Left radiographs show 3-dimensional position and orientation of the implant as measured by model-based shape-matching techniques. Right table shows articular surface separation and rotation between polyethylene insert and femoral component.

	Left	Right
Cum-Post distance	(-)*	(-)
Disengagement (med/lat) [mm]	(-)/0.99	(-)/0.21
Internal tibial rotation [degrees]	13.8	9.52

\*(-), below the lower detection limit